# A Mechanochemical Model of Growth Termination in Vertical Carbon Nanotube Forests

**Jae-Hee Han,[†] Rachel A. Graff,[†] Bob Welch,[‡] Charles P. Marsh,[§] Ryan Franks,[§] and Michael S. Strano[†,*]**

[†]Department of Chemical Engineering, Massachusetts Institute of Technology, 77 Massachusetts Avenue, Building 66-153, Cambridge, Massachusetts 02139-4307, [‡]U.S. Army Engineer Research and Development Center, Information Technology Laboratory, 3909 Halls Ferry Road, Vicksburg, Mississippi 39180-6199, and [§]U.S. Army Engineer Research and Development Center, Construction Engineering Research Laboratory, 2902 Newmark Drive, Champaign, Illinois 61822-1076

**ABSTRACT** Understanding the mechanisms by which vertical arrays of carbon nanotube (CNT) forests terminate their growth may lead to the production of aligned materials of infinite length. We confirm through calculation of the Thiele modulus that several prominent systems reported in the literature to date are not stunted by diffusion limitations. Evidence also suggests that, for many systems, the growth-termination mechanism is spatially correlated among nanotubes, making spontaneous, random catalytic poisoning unlikely as a dominant mechanism. We propose that a mechanical coupling of the top surface of the film creates an energetic barrier to the relative displacement between neighboring nanotubes. A Monte Carlo simulation based on this premise is able to qualitatively reproduce characteristic deflections of the top surface of single- and doubled-walled CNT (SWNT and DWNT) films near the edges and corners. The analysis asserts that the coupling is limited by the enthalpy of the carbon-forming reaction. We show that for patterned domains, the resulting top surface of the pillars is approximately conic with hyperbolic cross sections that allow for empirical calculation of a threshold force ($F_{max}$ = 34–51 nN for SWNTs, 25–27 nN for DWNTs) and elastic constant ($k$, 384–547 N/m for SWNTs and 157–167 N/m for DWNTs) from the images of experimentally synthesized films. Despite differences in nanotube type and precursor chemistry, the values appear consistent supporting the validity of the model. The possible origin of the mechanical coupling is discussed.

**KEYWORDS:** carbon nanotube · vertical film · vertical forest · growth termination mechanism · mechanical coupling · spatial correlation · covalently tethering

Densely packed, aligned, carbon nanotube (CNT) forests grown by chemical vapor deposition (CVD) have received significant attention of late because of their potential for applications in polymer–nanotube composites affording significantly anisotropic electrical, thermal, and mechanical properties.[1] Other potential applications include chemical and biological sensors,[2,3] supercapacitors,[4] fuel cells,[5] and thermally conducting interconnects for cooling electronic circuits[6] and mechanical structures.[7] They are of equal value for fundamental studies on semi-infinite, extended length arrays of nanoscale rods.[8,9] To this end, numerous attempts have been made in synthesizing (i) extended single-walled CNT (SWNT)[10]-, double-walled CNT (DWNT)[11]-, and multiwalled CNT (MWNT)[12]-dominant films, and (ii) laterally grown, prolonged individual SWNTs over flat[13] or trenched[9] Si wafers. For the latter, lengths have been reported up to 4–10 cm[9,13] often corresponding to the physical dimensions of the synthesis reactor. In contrast, vertical films are apparently limited in their growth by an unknown mechanism that terminates the process abruptly at a few tens[14,15] to hundreds micrometers,[16] or even up to 4.7 mm.[12] Our interest is in understanding growth termination of vertical CNT films with the ultimate goal of circumventing it to produce films of infinite thickness. We first rule out both diffusion limitations and spontaneous catalyst deactivation as dominant mechanisms of growth termination. We propose for the first time a chemical–mechanical coupling model to explain termination and show that it consistently describes several key observations reported in the literature for these systems.

**Diffusion Limitations Do Not Account for Sudden Growth Termination.** The argument that diffusion limitations are responsible for the abrupt reduction or termination of the growth rate is predicated on the idea that the carbon precursor must diffuse through the growing film to the base where reaction at catalytic nanoparticles extends the carbon film upward. The onset of diffusion limitations in a reacting system is predicted by calculation of the Thiele modulus $\varphi$–a dimensionless measure of the relative rates of reaction *versus* diffusion. In this particular geometry, for a constant growth rate $r_{rxn}$ (mol time$^{-1}$ area$^{-1}$), the Thiele modulus for a film grown under pressure $P$, temperature $T$, and thickness $z$ is

Ⓦ This paper contains enhanced objects available on the Internet at http://pubs.acs.org/journals/ancac3.

*Address correspondence to strano@mit.edu.

Received for review August 28, 2007 and accepted December 09, 2007.

**Published online January 22, 2008.**
10.1021/nn700200c CCC: $40.75

$$\varphi = \frac{n_c D_e P}{zRTr_{rxn}} \quad (1)$$

Here, $D_e$ is the effective diffusivity of the precursor gas in the growing film and $n_c$ is the number of carbon atoms per precursor molecule that react to create the film. The reaction rate is controlling as $\varphi \rightarrow \infty$. It can be shown that the maximum growth rate is that for which $\varphi = 1$ and that this represents the diffusion control limit. Using a typical growth rate, 0.1 mm/min and assuming a 1 nm nanotube pitch, a carbon consumption rate of $1 \times 10^{-8}$ mol $s^{-1}$ $m^{-2}$ is calculated. Zhu et al.[17] have estimated the effective diffusivity of ethylene in CNT films as $10^{-8}$ $m^2$ $s^{-1}$; hence at atmospheric pressure and reaction temperature range between 973 and 1173 K, $\varphi = 18.8–22.6$ for ethylene for a 1 m thick film. Therefore, typical growth conditions are kinetically controlled, and diffusion does not need to be considered. Recent experimental verifications of this fact support this conclusion.[12,18] It should also be noted that diffusion control, even if operative during growth, does not predict a complete termination of film growth.

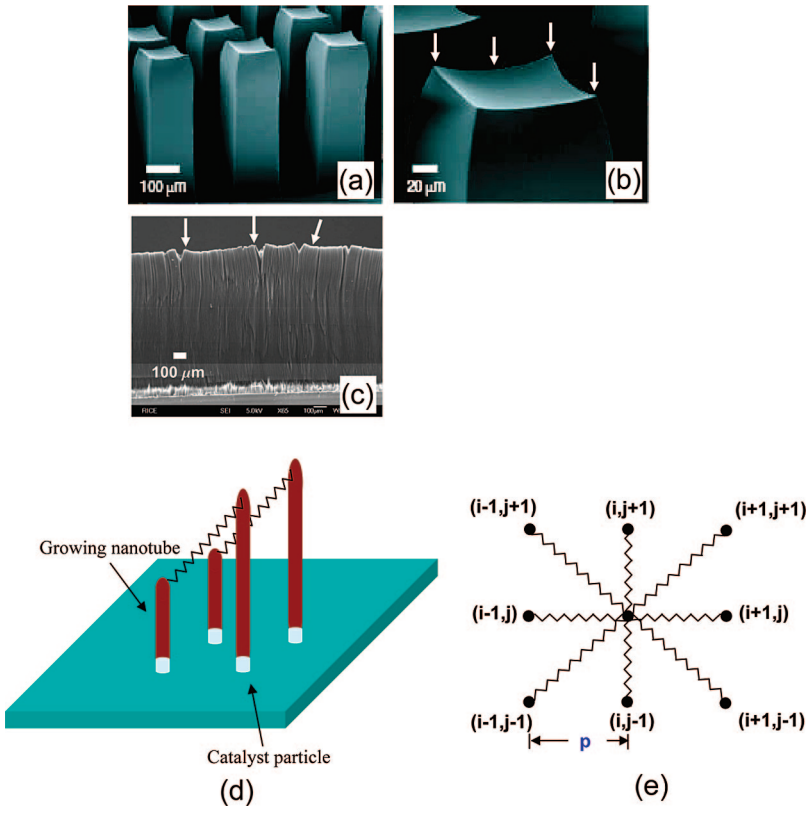


**Figure 1. (a) Expansive view from side and (b) magnified view from the top of SEM images of the designed macroscopic rectangular parallelepipeds of 2.2 mm DWNT forests grown by a water-assisted CVD method using 10–150 sccm $C_2H_4$ at 750 °C. Reprinted with permission from ref 11. Copyright 2006 Nature Publishing Group. (c) A SEM image of 1 mm vertically aligned SWNT forests grown by a hot filament CVD method with 400 sccm $H_2$ and 40 sccm $CH_4$ at 750 °C. Reprinted with permission from ref 20. Copyright 2006, American Institute of Physics. Arrows shown in Figure 1, panels b and c, indicate the deflection from center to end on the top surface as well as that on edges of the side of the film. (d) A schematic picture showing that each nanotube is mechanically coupled to neighboring members at the ends facing the growth direction, and (e) a projection view of the lattice of nanotubes modeled as connected springs.**

**Termination Is Spatially Correlated among Nanotubes.** A critical observation overlooked in the literature is the report that termination is spatially correlated. Hart and coworkers[19] used an *in situ* video imaging experiment to observe that termination does not occur uniformly across the film but rather in selected regions where the reaction first slows then stops. Evidence for the spatial correlation between nanotubes at growth termination is abundant. Figure 1, panels a and b, shows scanning electron microscopy (SEM) micrographs of patterned DWNT arrays with a characteristic deflection of the top surface (from ref 11). The same features are observable on SWNT films (Figure 1, panel c) from ref 20. Such surfaces are impossible in the absence of a spatial coupling between growing nanotubes. For example, random catalytic deactivation[21] cannot result in spatially correlated termination events. We assert that a valid termination mechanism must be consistent with this observation of correlated termination.

**A Mechanochemical Coupling Model of Growth Termination.** The spatial correlation in growth termination suggests a physical coupling between CNTs during growth. A mechanical coupling between independently growing CNTs can create an energy barrier that ultimately exceeds the energy available from chemical reaction at underlying catalyst particles. Using a simple elastic coupling of nanotubes at the exposed surface and assuming growth termination when the energy limit is reached, we demonstrate that a Monte Carlo simulation of the growing film reproduces the unique shape of the top surfaces observed experimentally (Figure 1, panels a–c). This model predicts that the characteristic shape is conic and, therefore, creates a hyperbolic curve when imaged in cross section, as with SEM. A simple geometric relation can then allow one to estimate molecular level parameters, such as the coupling spring constant or maximum vertical force, from this experimentally observed shape. We find that parameter values derived in this way for two different chemical precursors, leading to two different CNT types, are in agreement, supporting the generality of the mechanism. We also speculate about the nature of this mechanical coupling and note that the forces involved implicate chemical bonding.

**Literature Evidence Supporting Mechanical Coupling.** There are some recent references to mechanical forces influencing the growth of CNT films.[22,23] It is noted that an individual SWNT possesses a large elastic modulus (Young's modulus)[24] and tensile strength close to 1 TPa and 30 GPa, respectively.[25] Hart *et al.*[23] point out that the average force out-

put is 0.16 nN per CNT having outer diameter of 9 nm and five walls in their growth experiments, where a mechanical force applied to the growth site affected the morphology and growth rate of CNTs in a densely packed film. In their recent report, the time evolution of CNT growth using optical imaging revealed film cracking presumably due to spatial nonuniformities in growth rate and the resulting mechanical stresses.[19] Such cracking[26] or edge bending[10,11,27,28] in the vertical arrays of nanotube films either during or after growth stoppage appears generic and highly suggestive of mechanical stress in the film as a source of growth termination.

## RESULTS AND DISCUSSION

**Theoretical Modeling and Simulation.** ***The Termination Mechanism of Vertically Grown Nanotube Films.*** The shape of the top surface of some films frequently presents corners deflected upward (Figure 1, panels a–c). We hypothesize that this is a signature of a mechanical coupling between nanotubes only in or near the plane of this top surface. Consider the growth of a vertically aligned film of nanotubes equally spaced with pitch, $p$, in a regular, square lattice. Nanotubes grow upward from catalyst particles at the base, where a carbon-forming reaction extends the length at some characteristic rate. If the nanotubes are mechanically coupled to neighboring members at the ends facing the growth direction, the difference in height between a nanotube and its neighbors determines how much potential energy is stored within the couple. We can model this as a network of connected linear-elastic springs at the top of each nanotube, with proportionality between force and displacement equal to $k$, as depicted in Figure 1, panel d. The overall coupling scheme is given as shown in Figure 1, panel e, where the boundaries of the lattice are fixed (nonperiodic). The force on a nanotube at a position, $i$, $j$, in the lattice is then given by

$$F_{i,j} = k\sum_{n=-1}^{1}\sum_{m=-1}^{1}\left(\sqrt{\beta p^2 + (h_{i,j} - h_{i+m,j+n})^2} - \sqrt{\beta}p\right)$$

$$\begin{cases}\beta = 1 & m = 0 \quad \text{or} \quad n = 0\\ \beta = 2 & m \neq 0 \quad \& \quad n \neq 0\end{cases} \qquad (2)$$

Here, $h_{i,j}$ is the height at position $i,j$ and $\beta$ is a prefactor depending on the nanotube position in the lattice.

***Mechanical Coupling to the Growth Reaction at the Particle: An Energy Balance.*** This mechanical coupling has several implications. The most important is that there is a finite allowable displacement of one nanotube relative to another. Let us consider an energy balance on a growing nanotube with a catalyst particle at its base promoting the carbon-forming reaction. The chemical reaction provides energy for the physical displacement and upward growth of the nanotube. According to this model, without mechanical coupling of any kind, the nanotube would grow unbounded. However, the displacement of the nanotube relative to its neighbors requires the storage of potential energy within the mechanical couple. Formally, the chemical energy released by the reaction with the additional growth of one unit cell to the nanotube must be greater than or equal to the energy required to push the nanotube upward against the pull of neighboring nanotubes:

chemical energy released at particle = energy to extend nanotube $i,j$ upward relative to neighbors

$$n_{CNT}|\Delta H_{rxn}| \geq \int_{h_{ij}}^{h_{ij}+\delta} F(x)\,dx \approx F_{max}\delta \qquad (3)$$

Here, $n_{CNT}$ is the number of carbon atoms in a unit cell, $\delta$ is the height of the unit cell (m), and $\Delta H_{rxn}$ (in J/mol) is the heat of reaction at the reaction temperature per carbon basis of the growth reaction. The maximum difference in height between a nanotube and its neighbors is then finite, limited by the chemical energy driving the growth. The maximum force sustainable between coupled nanotubes is uniquely determined by the type of nanotube (the $(n,m)$ chirality) and the chemical reaction used for its production (Supporting Information contains an expression for $n_{CNT}/\delta$ in terms of $(n,m)$ for a SWNT).

We reason that the stress building up in the film does not apparently influence the growth rate at the base directly. Any negative feedback between the growth rate and the accumulated stress would necessarily self-correct (faster growing neighbors would subsequently minimize differences in height, resulting in no termination). Therefore, by this logic, growth termination is necessarily catastrophic. When the energy required to displace the nanotube upward exceeds a threshold set by the enthalpy of reaction for carbon formation according to eq 3, its growth stops. Neighboring nanotubes continue to grow but can be displaced only a finite distance before they too exceed this threshold $F_{max}$ and terminate growth. A circular wave of growth termination emanates from the termination point.

***Small Fluctuations in the Growth Rate.*** Also by this logic, if all of the nanotube growth rates are precisely equal, all nanotubes will have a net zero displacement relative to each other at all times and the film will grow infinitely. However, if we assume random variations in the growth rate $\pm\gamma$, where the parameter $\gamma$ is the fractional variation in growth rate, and we insist that $\gamma \ll 1$, small differences in growth rate when integrated over time would eventually yield one or more nanotubes exceeding the energy limit at some point, initiating the termination mechanism. This then produces a chain reaction as neighboring nanotubes continue to grow

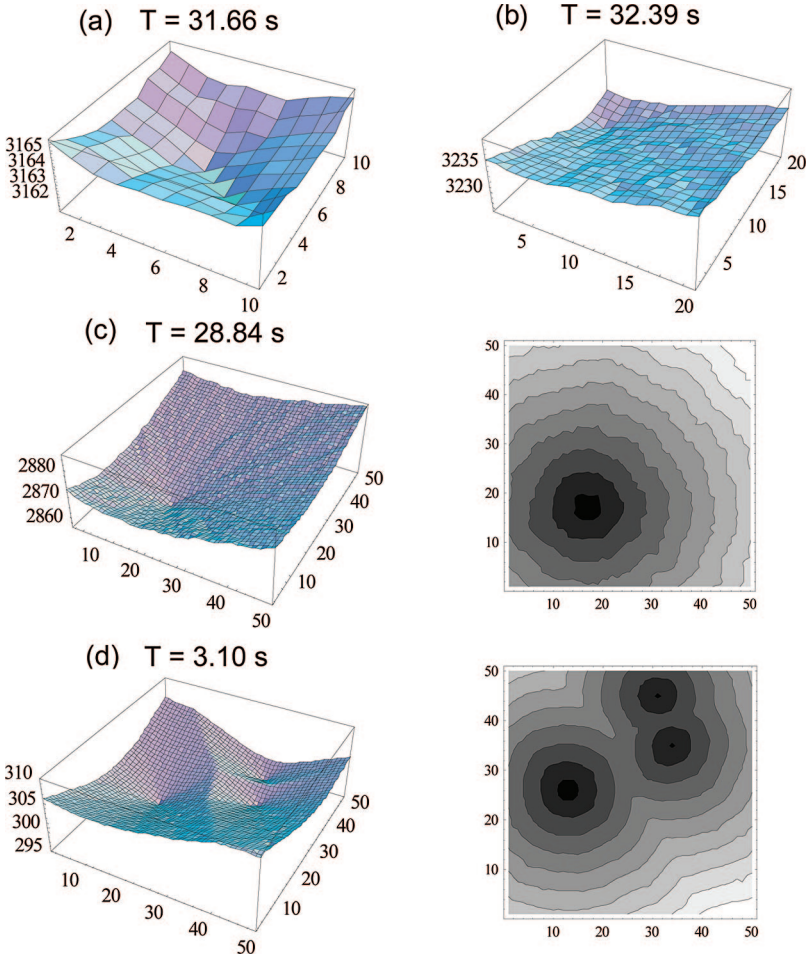


**Figure 2. Monte Carlo simulations of a growing vertical film as described in the text: (a) simulated 10 × 10 CNT array; (b) 20 × 20 array; (c) 50 × 50 array with resulting contour plot (right) showing a single termination site; (d) increasing γ to 0.5% creates multiple termination sites (right, contour plot) as observed for films of larger area. The time of growth termination is shown on the label, and all axes are in units of nanometers. Simulations employed a 2 nm pitch between nanotubes with an average rate of 100 nm/s and a variation, γ, of 0.005%. Mechanical coupling parameters were chosen at $F_{max}$ = 34 nN and $k$ = 384 N/m ($F_{max}/k$ = 0.088 nm). (See ref 20.)**

and also reach the critical limit. Formally, the simulation begins by selecting rates for each nanotube $i$, $j$

$$r_{i,j} = \bar{r}(1 + 2\gamma(\frac{1}{2} - \epsilon_{i,j})) \quad (4)$$

Here, $\epsilon_{i,j}$ is a continuous, random number between 0 and 1 assigned to the $(i,j)$ nanotube and $\bar{r}$ is the average growth rate of the vertical film chosen from literature values.

***Simulation Procedure.*** The simulation proceeds according to a simple scheme. The height of any nanotube is found by integrating the rate over the growth time, $t$:

$$h_{i,j} = r_{i,j}t \quad (5)$$

The algorithm steps in time, $t + \Delta t$, and continuously checks to see if $F_{i,j}$, has exceeded $F_{max}$. If it does, $r_{i,j}$ is set to 0 for this nanotube. The simulation process is terminated when rates for all nanotubes are zero.

Despite these simple rules, we find that the simulated films resemble those observed experimentally in several ways. Figure 2 shows the time evolution of growing films of vertically aligned nanotubes spaced 2 nm apart in pitch with average growth rate of 100 nm/s in arrays of 10 × 10, 20 × 20, and 50 × 50. The rate variation was chosen as 0.005%. This small variation value results in termination, occurs with a single nanotube, and radiates outwardly, creating the characteristic upturn of the film edges observed in DWNT films.[11] Increasing the domain size or increasing γ results in multiple termination centers (Figure 2, panel d, γ = 0.5%), as observed in refs 19 and 20. In cross section, the convex upward shape of Figure 2, panels a–c, is similar to SEM images of either patterned DWNT[11] or unpatterned SWNT[20] arrays in the literature. A representative movie is linked in the HTML version of Figure 3 demonstrating the outward radiation of growth termination that leads to the characteristic surface observed in experiments. An initial disparity in growth rates, although small, when integrated in time leads to a point or points of growth termination that spreads outward radially (Figure 3, panels a–e). Because the rates are assigned randomly, the epicenter of the propagation is not always restricted to the center of the array. This does appear to be consistent with experiments as a careful examination of Figure 1, panel a, shows that the minimum in the top surface does not occur exclusively at the geometric center. The model predicts that failure at the edge is unlikely, as nanotubes have fewer neighbors there and $F_{i,j}$ is always smaller.

***Relating Film Geometry to Fundamental Mechanical Properties.*** The ratio $F_{max}/k$ determines the final shape and height of the array and is related to both molecular and thermodynamic properties. According to this mechanism, the quantity $F_{max}$ is bounded by the enthalpy of reaction for the carbon forming chemistry and is easily calculated. The quantity $k$ is the spring constant of the unknown coupling and must be measured directly. Figure 4 shows that $F_{max}/k$ is related to the minimum and maximum dimension of the top surface of the array. As the ratio increases, the upward deflection becomes more prominent.

From geometry, one can show that the surface approximates a regular cone emanating from the first nanotube where growth terminates. The curvature at the cross section is then a hyperbola. On examination of this side face of the film, $w$ is the distance from the edge to the minimum at the center, and $a$ is the difference in height from this edge to the minimum. The ratio $a/w$

can be related to the maximum height difference experienced by two neighboring nanotubes before termination. From geometry, as shown in Figure 4, this height difference, $h_{max}$, is a function of $F_{max}/k$ and the nanotube pitch

$$h_{max} = \sqrt{\left(\frac{F_{max}}{k} + p\right)^2 - p^2} \quad (6)$$

The ratio $a/w$ can be written in terms of the fundamental mechanical properties, $F_{max}/k$

$$\left(\frac{a}{w}\right) = (\sqrt{2} - 1)\frac{\sqrt{(F_{max} + p)^2 - p^2}}{p} \quad (7)$$

Solving for $F_{max}/k$ *versus* $a/w$

$$\frac{F_{max}}{k} = p(\sqrt{1 + (3 + 2\sqrt{2})(a/w)^2} - 1) \quad (8)$$

Hence, one can carefully image (see Figure 1, panels a–c) the deflection of the film in cross section such that $a/w$ is measured, and *via* eq 8 the quantity $F_{max}/k$ can be estimated. We note that this parameter ratio should be temperature dependent (*via* temperature dependences of elastic and thermodynamic properties) and should vary considerably depending upon on the carbon precursor chemistry employed since $\Delta H_{rxn}$ is an inherent limitation on $F_{max}$.

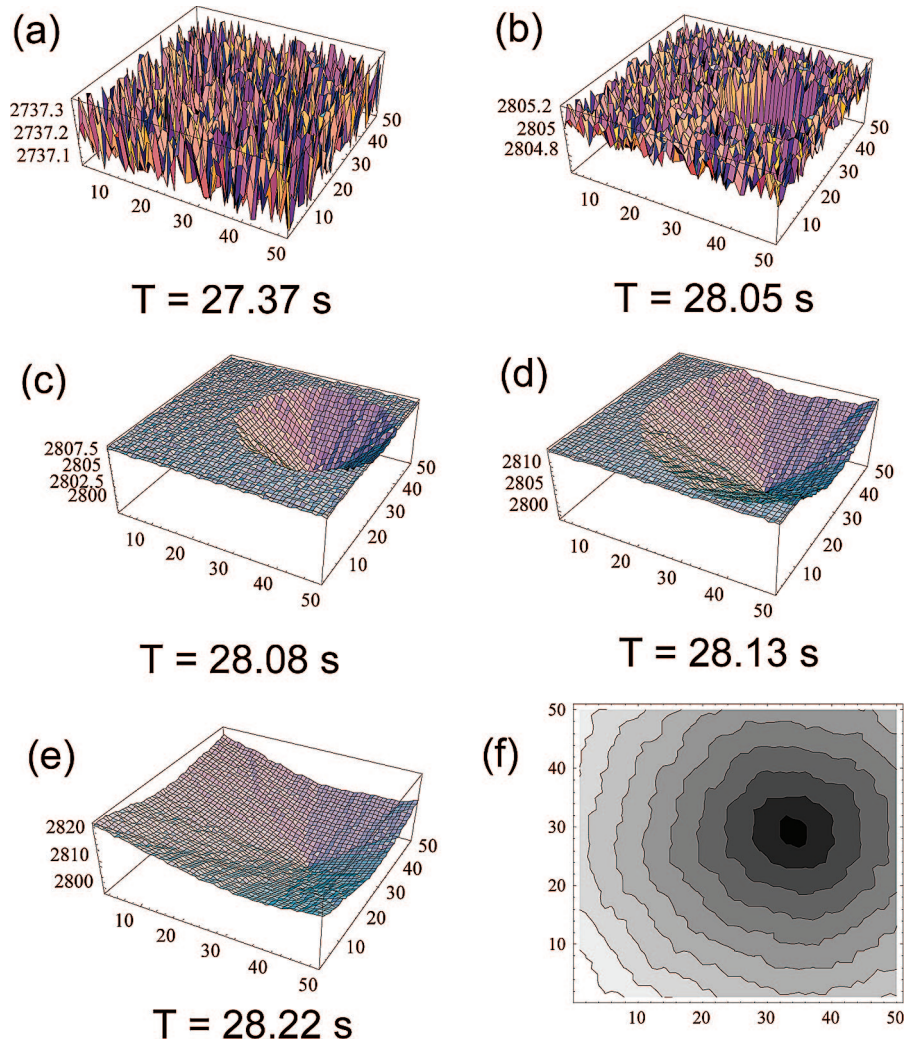


**Figure 3. Snapshots in time from a simulation of a vertically growing nanotube film (50 × 50 array) $F_{max}/k$ = 0.088 nm, showing an average height of 2.8 μm (γ = 0.005%, average growth rate = 100 nm/s) demonstrating the mechanism. The vertical array grows with increasing distances between neighboring nanotubes until the required work for further displacement exceeds the energy available at the catalyst particle for typically one nanotube (a). The halted growth of one exerts the same mechanism on neighbors creating a small fissure in the film (b). The fissure grows and propagates outward radially (c). At subsequent times, the shape is apparent as conic (d) and leads to a final contour the mimics what is observed experimentally when all growth stops at $T$ = 28.22 s (e). A contour plot depicts the radial propagation of the initial event near the center of the array (f).**

**Ⓦ A representative video in avi format demonstrating the outward radiation of growth termination that leads to the characteristic surface observed in experiments is available.**

## DISCUSSION

In this article, we use literature images to measure the ratios of $a/w$ for both the grown DWNT[11] and SWNT[20] films. The former yields approximately 0.126 and the latter 0.17, respectively. With eq 8 shown above, these values allow us to have the corresponding $F_{max}/k$ as $1.62 \times 10^{-10}$ and $9.05 \times 10^{-11}$ m, respectively. In order to calculate the upper bound for $F_{max}$ for each case, we used eq 3 and the known values of $n_{SWNT}$ and δ for a given ($n$,$m$) nanotube,[29] and $\Delta H_{rxn}$ calculated from the thermodynamic properties of each type of carbon feedstock (ethylene ($C_2H_4$) for ref 11 and acetylene ($C_2H_2$) for ref 20,[30] respectively) at the reaction temperatures (750 °C for both). It must be noted that the authors of the ref 20 demonstrated that by turning a tungsten hot filament on during the

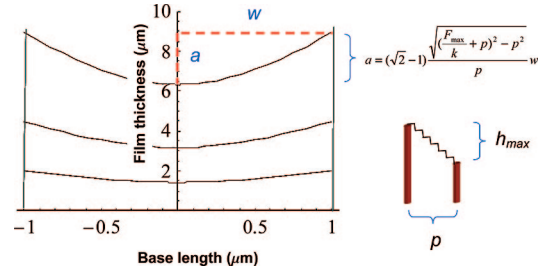


**Figure 4. The geometry of the top of the film can be utilized to estimate the extent of mechanical coupling. The cross section of the film can be shown to approximate a hyperbolic function with axes related to the ratio $F_{max}/k$. A geometric relation (shown) can relate measurable dimensions to this ratio. Here, $w$ is the distance from the edge to the minimum at the center and $a$ is the difference in height from the edge to the center.**

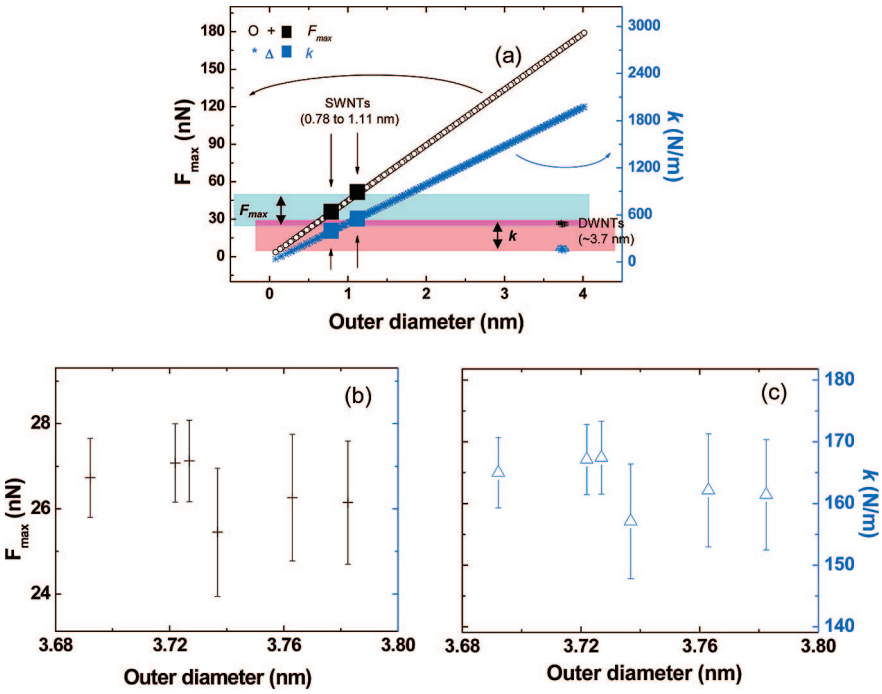


**Figure 5. (a) A combined plot of both $F_{max}$ (left axis, indicated by black open circles and crosses) and $k$ (right axis, indicated by blue asterisks and triangles) *vs* nanotube outer diameters. Each black and blue solid rectangle indicates the corresponding actual points of $F_{max}$ and $k$ for SWNTs ($d$ = 0.78 and 1.11 nm).[20] Also $F_{max}$ and $k$ for SWNTs at each diameter are found to be 34 nN and 384 N/m ($d$ = 0.78 nm), and 51 nN and 547 N/m ($d$ = 1.11 nm), respectively. Values for $F_{max}$ were estimated from the energy balance of eq 3, and $k$ was then calculated from the hyperbolic geometry (eq 8). For two different chemistries published in the literature, producing two different CNT types (single- and double-walled), it is noteworthy that values cluster within a factor of 2 indicating similar termination mechanisms. Expanded plots (b) for $F_{max}$ and (c) for $k$ *vs* nanotube outer diameter for ~3.7 nm diameter DWNTs[11] show mean values of $F_{max}$ (25–27 nN) and $k$ (157–167 N/m) for ~3.7 nm diameter DWNTs, respectively.**

growth period, a small amount of $CH_4$[30] was converted into both acetylene ($C_2H_2$) and $C_2H_4$ (experimentally confirmed by *in situ* FT-IR in their system). From their experimental results with FT-IR, they found that the SWNTs growth occurred only when the filament was turned on hot enough to decompose $CH_4$ into $C_2H_2$ (regarded as main carbon source with ~30% contribution to growth) and $C_2H_4$ with possible minority of methyl radical. These molecules are believed to produce the active carbon precursors for SWNT growth so that small diameter SWNT films are formed. Therefore, in this work, we used value of $\Delta H_{rxn}$ of $C_2H_4$ ($-3.86 \times 10^4$ J/mol) for ref 11 and approximated that by just $C_2H_2$ ($-2.24 \times 10^5$ J/mol), instead of $CH_4$[30] for ref 20, respectively, to estimate $F_{max}$.

With the ratios of $a/w$ measured from literature images, a combined plot for both $F_{max}$ and $k$ *versus* nanotube outer diameters can be constructed as in Figure 5. In ref 11, the authors report that DWNT-dominant films of individual mean diameter of ~3.7 nm were synthesized under the optimized experimental condition. As shown in Figure 5, mean values of $F_{max}$ (25–27 nN) and $k$ (157–167 N/m) for ~3.7 nm diameter DWNTs can be estimated, respectively. In ref 20, the authors obtained small diameter SWNTs films with individual diameters ranging from 0.78 to 1.11 nm. Also $F_{max}$ and $k$ for SWNTs at each diameter on two linear plots (designated as open circles and asterisks, respectively) are found to be 34 nN and 384 N/m ($d$ = 0.78 nm), and 51 nN and 547 N/m ($d$ = 1.11 nm), respectively. It is notable that despite differences in carbon feedstock and nanotube diameters, values for both $F_{max}$ and $k$ are similar (Figure 5, panel a, blue and red rectangles). This fact demonstrates that our qualitative hypothesis asserted in this article does rationally make sense. It is not clear why $F_{max}$ and $k$ are larger for SWNTs than for DWNTs. One possibility is the difference in elastic properties as additional wall layers increase Young's modulus[31] (or bending stiffness[32]). Stored mechanical energy from the growing neighboring nanotubes of the higher Young's modulus (or bending stiffness) should be greater, leading to higher $F_{max}$ and $k$. However it is not clear how the degrees of bundling, chirality, and structural defects influence the energetics.

**On the Origin of the Mechanical Coupling.** There are several possibilities as to the source of this coupling. One is that van der Waals (VDW) contact between ends near the top surface of the growing film restricts the growth of one nanotube relative to another. In order to calculate the contribution of the VDW interaction along the length of neighboring nanotubes to the CNT growth termination, we used a continuum model[33,34] based on the atomistic Lennard-Jones (LJ) potential.[35] The potential between two identical, parallel nanotubes is characterized by

$$\varphi(R) = \sigma^2 \int u(x)\, d\Sigma_1\, d\Sigma_2 \qquad (9)$$

Here, $\sigma$ is the mean surface density of carbon atoms and $x$ is the distance between two surface elements $d\Sigma_1$ and $d\Sigma_2$ on two different nanotubes (see Supporting Information). Following prior work,[35] we studied CNTs for which the VDW interaction is averaged along the tube surface. Such a model gives the minimum VDW interaction energy per unit length at each equilibrium interaction distance to the SWNT (0.11 to 0.14 nN for $d$ = 0.78–1.11 nm, respectively)[20] and DWNT (0.25–0.26 nN for $d$ = 3.7 nm)[11] (see Supplementary Figure S1). Just beyond this equilibrium distance (*e.g.*, 1.08–1.41 nm for SWNTs ($d$ = 1.08–1.11 nm) and 4.04–4.1 nm for DWNTs ($d$ = 3.7 nm), respectively), the VDW force increases asymmetrically and rapidly as expected. Note

that these VDW force values for both SWNTs and DWNTs are approximately 2 orders of magnitude lower than $F_{max}$ (34–51 nN for SWNTs, and 29 nN for DWNTs, respectively). Also it is worth mentioning that from theory, the minimum VDW interaction energy simply varies with nanotube diameter, but $F_{max}$ appears to be independent of the type of nanotube, its diameter, or even the feedstock used for synthesis.

Another possibility is simply the sliding resistance of two parallel nanotubes. Several reports[36–38] describe the interlayer sliding force of graphene due to the VDW interaction energy for telescoping DWNT or MWNT. The force was estimated or experimentally measured (*ca.* 9–10 nN) using nanomanipulation (*e.g.*, atomic force microscope tip), based on the configuration of the extraction and restoration of inner core–shell in the coaxial nanotube. Since such force is estimated basically using the graphene–graphene interlayers (not intertube) distance (*ca.* 0.34 nm); however, this force would become quite small (a few tens to hundreds of piconewton) if the intertube distance increased.

A third option is covalent tethering at the top of the nanotube to adjacent nanotubes. In this case, dangling bonds present at the potentially open nanotube end could cross-link, covalently tethering adjacent nanotubes. It is noted that the magnitude of force constants for chemical bond stretching in organic molecules[39]—for example, C–H (448 N/m) in CH, C–H (544 N/m) in $CH_4$, and C–C (1216 N/m) in $C_2$—are close to the same order of those in our calculated values for elastic constants *k* (384–547 N/m for SWNTs and 157–167 N/m for DWNTs). Despite experimental uncertainties in the determination of $F_{max}$ (and *k*), this possibility is most consistent with our calculations.

## CONCLUSION

We show that this characteristic yet unexplained deflection of the top surface of vertically aligned CNT films can be explained by a mechanical coupling between neighboring nanotubes. A Monte Carlo simulation of film growth is able to qualitatively reproduce the shape by assuming that the coupling is limited by the thermodynamics of the carbon forming reaction. The shape of the surface is approximately conic with hyperbolic cross sections that allow for the calculation of a threshold force ($F_{max}$ = 34–51 nN for SWNT, 25–27 nN for DWNT) and elastic constant (*k*, 384–547 N/m for SWNT and 157–167 N/m for DWNT) from the images of experimentally synthesized films. Note that these values are for specific examples of growth considered in this work. Despite differences in nanotube type and precursor chemistry, the values appear consistent supporting the model. The origin of the mechanical coupling is not fully understood but is likely covalent in nature and possibly arises from the reaction of dangling bonds on growing nanotubes.

## METHODS

**Materials.** In order to reproduce and calculate $F_{max}$ and *k*, the cross-sectional images of vertically grown forests of both DWNTs[11] and SWNTs[20] from the literature were used.

**Simulation.** The Monte Carlo simulation of the growing film reproducing the unique shape of the top surfaces observed experimentally was performed through Mathematica (Ver. 5.2).

*Acknowledgment.* This work was funded by a grant from the Air Force Office of Sponsored Research (Multi-Functional Materials), an NSF Career Award and 3M Untenured Faculty Award to M.S.S, and a grant from Army Research Labs to the Construction Engineering Research Laboratory (C. P. Marsh). J.H.H. acknowledges support by the Postdoctoral Research Program of Sungkyunkwan University (2005).

*Supporting Information Available:* An example for the calculation procedure of $F_{max}$ and an additional estimation and the corresponding figure of the VDW interaction between two identical, parallel nanotubes utilized in this work. This material is available free of charge *via* the Internet at http://pubs.acs.org.

## REFERENCES AND NOTES

1. Coleman, J. N.; Khan, U.; Gun'ko, Y. K. Mechanical reinforcement of polymers using carbon nanotubes. *Adv. Mater.* **2006**, *18*, 689–706.
2. Wei, C.; Dai, L.; Roy, A.; Tolle, T. B. Multifunctional chemical vapor sensors of aligned carbon nanotube and polymer composites. *J. Am. Chem. Soc.* **2006**, *128*, 1412–1413.
3. Li, J.; Koehne, J. E.; Cassell, A. M.; Chen, H.; Ng, H. T.; Ye, Q.; Fan, W.; Han, J.; Meyyappan, M. Inlaid multi-walled carbon nanotube nanoelectrode arrays for electroanalysis. *Electroanalysis* **2005**, *17*, 15–27.
4. Lee, Y. H.; An, K. H.; Lee, J. Y.; Lim, S. C. Carbon nanotube-based supercapacitors. In *Encyclopedia of Nanoscience and Nanotechnology*; Nalwa, H., Ed.; American Scientific Publishers: Stevenson Ranch, CA, 2004; Vol. 1, pp 625–634.
5. Yildirim, T.; Ciraci, S. Titanium-decorated carbon nanotubes as a potential high-capacity hydrogen storage medium. *Phys. Rev. Lett.* **2005**, *94*, 175501.
6. Kreupl, F.; Graham, A. P.; Duesberg, G. S.; Steinhögl, W.; Liebau, M.; Unger, E.; Hönlein, W. Carbon nanotubes in interconnect applications. *Microelectron. Eng.* **2002**, *64*, 399–408.
7. Yakobson, B. I.; Smalley, R. E. Fullerene nanotubes: C-1000000 and beyond. *Am. Sci.* **1997**, *85*, 324–337.
8. Li, S.; Yu, Z.; Rutherglen, C.; Burke, P. J. Electrical properties of 0.4 cm long single-walled carbon nanotubes. *Nano Lett.* **2004**, *4*, 2003–2007.
9. Hong, B. H.; Lee, J. Y.; Beetz, T.; Zhu, Y.; Kim, P.; Kim, K. S. Quasi-continuous growth of ultralong carbon nanotube arrays. *J. Am. Chem. Soc.* **2005**, *127*, 15336–15337.
10. Hata, K.; Futaba, D. N.; Mizuno, K.; Namai, T.; Yumura, M.; Iijima, S. Water-assisted highly efficient synthesis of impurity-free single-walled carbon nanotubes. *Science* **2004**, *306*, 1362–1364.
11. Yamada, T.; Namai, T.; Hata, K.; Futaba, D. N.; Mizuno, K.; Fan, J.; Yudasaka, M.; Yumura, M.; Iijima, S. Size-selective growth of double-walled carbon nanotube forests from engineered iron catalysts. *Nat. Nanotechnol.* **2006**, *1*, 131–136.
12. Li, Q.; Zhang, X.; DePaula, R. F.; Zheng, L.; Zhao, Y.; Stan, L.; Holesinger, T. G.; Arendt, P. N.; Peterson, D. E.; Zhu, Y. T. Sustained growth of ultralong carbon nanotube arrays for fiber spinning. *Adv. Mater.* **2006**, *18*, 3160–3163.

13. Zheng, L. X.; O'connell, M. J.; Doorn, S. K.; Liao, X. Z.; Zhao, Y. H.; Akhadov, E. A.; Hoffbauer, M. A.; Roop, B. J.; Jia, Q. X.; Dye, R. C.; Peterson, D. E.; Huang, S. M.; Liu, J.; Zhu, Y. T. Ultralong single-wall carbon nanotubes. *Nat. Mater.* **2004**, *3*, 673–676.
14. Andrews, R.; Jacques, D.; Qian, D.; Rantell, T. Multiwall carbon nanotubes: synthesis and application. *Acc. Chem. Res.* **2002**, *35*, 1008–1017.
15. Murakami, Y.; Chiashi, S.; Miyauchi, Y.; Hu, M.; Ogura, M.; Okubo, T.; Maruyama, S. Growth of vertically aligned single-walled carbon nanotube films on quartz substrates and their optical anisotropy. *Chem. Phys. Lett.* **2004**, *385*, 298–303.
16. Geohegan, D. B.; Puretzky, A. A.; Ivanov, I. N.; Jesse, S.; Eres, G.; Howe, J. Y. In situ growth rate measurements and length control during chemical vapor deposition of vertically aligned multiwall carbon nanotubes. *Appl. Phys. Lett.* **2003**, *83*, 1851–1853.
17. Zhu, L.; Hess, D. W.; Wong, C.-P. Monitoring carbon nanotube growth by formation of nanotube stacks and investigation of the diffusion-controlled kinetics. *J. Phys. Chem. B* **2006**, *110*, 5445–5449.
18. Zhu, L.; Xu, J.; Xiao, F.; Jiang, H.; Hess, D. W.; Wong, C. P. The growth of carbon nanotube stacks in the kinetics-controlled regime. *Carbon* **2007**, *45*, 344–348.
19. Hart, A. J.; van Laake, L.; Slocum, A. H. Desktop growth of carbon-nanotube monoliths with in situ optical imaging. *Small* **2007**, *3*, 772–777.
20. Xu, Y.-Q.; Flor, E.; Schmidt, H.; Smalley, R. E.; Hauge, R. H. Effects of atomic hydrogen and active carbon species in 1 mm vertically aligned single-walled carbon nanotube growth. *Appl. Phys. Lett.* **2006**, *89*, 123116.
21. Futaba, D. N.; Hata, K.; Yamada, T.; Mizuno, K.; Yumura, M.; Iijima, S. Kinetics of water-assisted single-walled carbon nanotube synthesis revealed by a time-evolution analysis. *Phys. Rev. Lett.* **2005**, *95*, 056104.
22. Hart, A. J.; Slocum, A. H. Rapid growth and flow-mediated nucleation of millimeter-scale aligned carbon nanotube structures from a thin-film catalyst. *J. Phys. Chem. B* **2006**, *110*, 8250–8257.
23. Hart, A. J.; Slocum, A. H. Force output, control of film structure, and microscale shape transfer by carbon nanotube growth under mechanical pressure. *Nano Lett.* **2006**, *6*, 1254–1260.
24. Yu, M.-F. Fundamental mechanical properties of carbon nanotubes: current understanding and the related experimental studies. *J. Eng. Mater. Technol.* **2004**, *126*, 271–278.
25. Yu, M.-F.; Files, B. S.; Arepalli, S.; Ruoff, R. S. Tensile loading of ropes of single wall carbon nanotubes and their mechanical properties. *Phys. Rev. Lett.* **2000**, *84*, 5552–5555.
26. Puretzky, A. A.; Geohegan, D. B.; Jesse, S.; Ivanov, I. N.; Eres, G. In situ measurements and modeling of carbon nanotube array growth kinetics during chemical vapor deposition. *Appl. Phys. A: Mater. Sci. Process.* **2005**, *81*, 223–240.
27. Zhang, G.; Mann, D.; Zhang, L.; Javey, A.; Li, Y.; Yenilmez, E.; Wang, Q.; McVittie, J. P.; Nishi, Y.; Gibbons, J.; Dai, H. Ultra-high-yield growth of vertical single-walled carbon nanotubes: hidden roles of hydrogen and oxygen. *Proc. Natl. Acad. Sci. U.S.A.* **2005**, *102*, 16141–16145.
28. Noda, S.; Hasegawa, K.; Sugime, H.; Kakehi, K.; Zhang, Z.; Maruyama, S.; Yamaguchi, Y. Millimeter-thick single-walled carbon nanotube forests: hidden role of catalyst support. *Jpn. J. Appl. Phys.* **2007**, *46*, L399–L401.
29. Saito, R.; Dresselhaus, G.; Dresselhaus, M. S. *Physical Properties of Carbon Nanotubes*; Imperial College Press: London, 1998. Note that for calculation of $n_{SWNT}$ and $\delta$ of ~3.7 nm diameter DWNTs, the structural properties of possible inner diameter SWNTs, which have typically 0.66–0.82 nm diameters less than the outer one (~3.7 nm), were taken into account as well. Also see Supporting Information.
30. The authors of ref 20 originally used $CH_4$ (not $C_2H_2$) as carbon feedstock for the SWNT growth. In this article, however, we used the thermodynamic value of $C_2H_2$ (see the text for relevant reason). Since we assumed that the chemical energy released by the reaction provides energy for the physical displacement and upward growth of the nanotube, this reaction process should be exothermic. Note that the dissociation reaction of $CH_4$ ($C_2H_2$) is an endothermic (exothermic) process so that it requires (releases) heat from (to) the system.
31. Yao, N.; Lordi, V. Young's modulus of single-walled carbon nanotubes. *J. Appl. Phys.* **1998**, *84*, 1939–1943.
32. Ru, C. Q. Effective bending stiffness of carbon nanotubes. *Phys. Rev. B* **2000**, *62*, 9973–9976.
33. Girifalco, L. A.; Lad, R. A. Energy of cohesion, compressibility, and the potential energy functions of the graphite system. *J. Phys. Chem.* **1956**, *25*, 693–697.
34. Girifalco, L. A.; Hodak, M.; Lee, R. S. Carbon nanotubes, buckyballs, ropes, and a universal graphitic potential. *Phys. Rev. B* **2000**, *62*, 13104–13110.
35. Lennard-Jones, J. E. Perturbation problems in quantum mechanics. *Proc. R. Soc. London, Ser. A* **1930**, *129*, 598–615.
36. Cumings, J. A.; Zettle, J. Low-friction nanoscale linear bearing realized from multiwall carbon nanotubes. *Science* **2000**, *289*, 602–604.
37. Zheng, Q.; Liu, J. Z.; Jiang, Q. Excess van der Waals interaction energy of a multiwalled carbon nanotube with an extruded core and the induced core oscillation. *Phys. Rev. B* **2002**, *65*, 245409.
38. Akita, S.; Nishijima, H.; Kishida, T.; Nakayama, Y. Influence of force acting on side face of carbon nanotube in atomic force microscopy. *Jpn. J. Appl. Phys.* **2000**, *39*, 3724–3727.
39. Lide, D. R. *CRC Handbook of Chemistry and Physics*, 76th ed.; CRC Press: Boca Raton, FL, 1995–1996; pp 9–74.